



**HAL**  
open science

# The Influence of Physical Parameters on Space Charge Accumulation and Phase Characteristics in Cable Insulation under ac Electric Field

Dongxin He, Zhe Xu, Hongshun Liu, Qingjing Zang, Qingquan Li, Séverine Le Roy, Gilbert Teyssedre

► **To cite this version:**

Dongxin He, Zhe Xu, Hongshun Liu, Qingjing Zang, Qingquan Li, et al.. The Influence of Physical Parameters on Space Charge Accumulation and Phase Characteristics in Cable Insulation under ac Electric Field. IEEE Transactions on Industry Applications, 2022, 58 (1), pp.59-66. 10.1109/TIA.2021.3119539 . hal-03784684

**HAL Id: hal-03784684**

**<https://hal.science/hal-03784684>**

Submitted on 23 Sep 2022

**HAL** is a multi-disciplinary open access archive for the deposit and dissemination of scientific research documents, whether they are published or not. The documents may come from teaching and research institutions in France or abroad, or from public or private research centers.

L'archive ouverte pluridisciplinaire **HAL**, est destinée au dépôt et à la diffusion de documents scientifiques de niveau recherche, publiés ou non, émanant des établissements d'enseignement et de recherche français ou étrangers, des laboratoires publics ou privés.

# The Influence of Physical Parameters on Space Charge Accumulation and Phase Characteristics in Cable Insulation under ac Electric Field

Dongxin He, Zhe Xu, Hongshun Liu, Qingjing Zang and Qingquan Li

Shandong Provincial Key Laboratory of UHV Transmission Technology and Equipment, School of Electrical Engineering, Shandong University, Jinan 250061, China

S  verine Le Roy and Gilbert Teyss  dre

University of Toulouse; UPS, INPT, CNRS; LAPLACE (Laboratoire Plasma et Conversion d'nergie); 118 Route de Narbonne, F-31062 Toulouse Cedex 9, France

**Abstract** - The space charge dynamic behavior and accumulation are important contributions to electrical tree aging, as recognized for crosslinked polyethylene (XLPE) cable insulation under alternating current (ac) electric stress. In this paper, in order to investigate the reason for the charge accumulation phenomenon revealed by experiments under ac stress, a bipolar space charge transport model with symmetrical or asymmetrical parameters is resolved under ac stress. The charge accumulation mechanism is analyzed based on position and amount of charge function of voltage application time and voltage phase. The effects of each major physical parameter are simulated and analyzed separately. It is found that there is no obvious accumulation of space charges with symmetrical parameters. Asymmetrical parameters result in a difference of motion process between positive and negative charges, which greatly enhances charge accumulation. Each main parameter has an influence on charge accumulation from different angles and levels. The applicability of the simulation model with asymmetrical parameters is assessed by comparing experiments and simulation results on space charge. This study contributes to the understanding of space charge generation mechanism under ac conditions and helps improving the stability and operation properties of XLPE cables in power system.

Index Terms — ac electric field, crosslinked polyethylene, space charge, accumulation characteristics, phase characteristics, physical parameters

## 1 INTRODUCTION

CROSS-LINKED polyethylene-insulated cables are widely used in underground power transmission systems of urban power grids because of their high electrical strength, low dielectric loss, good heat resistance, aging resistance and easy installation. Studies have shown that even when the electric field intensity applied for polymer insulation is much lower than the breakdown field of the insulation, cables operating for a long time are still subjected to electrical tree, which results in insulation breakdown. The formation and action of space charges are important factors to initiate electrical tree [1]. In the long-time running process of the

cable, space charges accumulate gradually near the electrodes, resulting in serious local electric field distortion which is an important reason for electrical tree [2,3]. Therefore, it is significant to explore accumulation characteristics and influencing factors of space charges in XLPE cable insulation.

The motion mechanism and accumulation characteristics of space charges in direct current (dc) electric field have been studied deeply and elaborately [4,5]. However, due to the limitations of time-matched measurement technology, space charge researches are scarcely treated under ac field. The existence of space charges in ac field has already been confirmed by the experimental measurements in some researches [6,7]. In these papers, space charge accumulation and its specific behavior with phase were investigated [8,9]. The experimental results show that there are two superimposed charge behaviors in the insulating materials under the ac electric field: charges having a periodic dynamic and charges having a non-periodic dynamic [8-10]. Periodic charges are generated by polarization, and the charge density varies with the amplitude and phase of the voltage. By definition, periodic charges do not accumulate. Non-periodic charges are generated by electrode injection and ionization and accumulate with the operation and aging of the cable. Compared with periodic charges, non-periodic charges have more far-reaching influence on cable performance. Therefore, this paper is focused on exploring the characteristics of non-periodic space charges.

The dynamic behavior of ac space charges is very difficult to measure experimentally, as a large amount of data need to be stored as a function of the period of stress. In order to explore the space charges dynamic, researchers have built numerical simulation models. Alison and Hill proposed a bipolar space charge transport model and described the space charges behavior under dc electric field [11]. G. Chen *et al* applied it to ac electric field, focusing on exploring the phase characteristics of space charges in a single voltage cycle [12]. Baudoin *et al* compared the variation law of space charges with phase obtained by simulation with the electroluminescence phenomenon measured by experiment. They verified that electroluminescence is closely related to the dynamic behaviors such as injection and recombination [13]. In order to reflect the

actual situation of the cable, Le Roy *et al* proposed a model taking into account the cylindrical geometry and researched the effect of the cylindrical geometry on the space charge profiles [14]. The above research analyzed the influence of space charges on insulation performance from different aspects. However, parameter selection is still unclear and the same parameters can have different values in the cited researches, therefore leading to uncertainties in the space charge generation and accumulation mechanisms.

Some researches have reported differences in the motion mechanism of positive and negative charges [14,15]. Under dc electric field, the difference between positive and negative charges only affects charge density in the moment when positive and negative charges meet in the process of moving towards opposite electrode. However, under ac electric field, positive and negative charges interact during each half voltage period. Therefore, the difference in the motion mechanism of positive and negative charges has a great impact. Hence compared with the dc stress, it is more necessary to explore the influence of asymmetrical physical parameters of the charge transport model on the charges under ac electric field. This can be performed through the comparison with the measured ac space charge measurements.

In this paper, charge accumulation under ac electric field is studied through experiment. Space charge experimental results are then compared to results issued from a bipolar space charge transport model, with symmetrical and asymmetrical parameters. The influence of four physical parameters on the charge accumulation characteristics is analyzed finally. The research will help improve the stability and operation properties of XLPE cables.

## 2 EXPERIMENTAL MEASUREMENT

### 2.1 PRINCIPLES AND CONDITIONS OF THE EXPERIMENT

Space charge measurement method under ac electric field have already been reported and only brief outline is given here [10]. A space charge measurement system based on the pulsed electro-acoustic method (PEA) was established. An ac phase matching circuit was designed to solve the problem in matching measurement time with phase of the 50 Hz sine voltage. Using this circuit, the ac sine signal is converted into 32 synchronized short square wave signals and the trigger time of high-frequency pulse voltage source is controlled. Space charge waveforms were produced by averaging more than 500 sinusoidal periods in one time, and the averaged space charge profiles in 32 phase angles were achieved with an interval of  $11.25^\circ$  [16].

The material under study is an XLPE cut and peeled from a cable having endured an accelerated aging under ac electric field for 200 days at the temperature of  $114^\circ\text{C}$  and the voltage of 26.1 kV. The XLPE peelings have a thickness of 230  $\mu\text{m}$  with an area of  $45 \times 45 \text{ mm}^2$ . Prior to any further measurement, the material is put in short-circuit for a long time to make charges dissipate. An ac electric field of 50Hz and 35kV/mm (root mean square value) was then applied to the slices for 6 hours, at  $25^\circ\text{C}$ .

## 2.2 MEASUREMENT RESULTS

The charges measured directly in the experiment include periodic charges and non-periodic charges [17]. The amplitude and polarity of periodic charges change with the voltage sign in a period. The density is the largest at  $90^\circ$  and  $270^\circ$  and the lowest at  $0^\circ$  and  $180^\circ$  respectively. We then choose to present the changes in charge density at  $90^\circ$  and  $270^\circ$  in the process of voltage application. Figure 1 presents the space charge profiles at these two phases, for different times under voltage. Generally, there is a formation of hetero-charges at the left electrode. The sign of the charges in the bulk and at the left electrode is positive when the electrode is negative, and the bulk becomes negative when the electrode becomes positive. As the piezoelectric sensor is located at the left electrode, the sensitivity is lowered at the right electrode, preventing any refined analysis. At a depth of about 25  $\mu\text{m}$  away from the left electrode, the positive charge density at  $90^\circ$  (electrode being cathode) decreases gradually, and the negative charge density at  $270^\circ$  (electrode being anode) increases gradually. This is also reflected on the electrode image charges. These results show that there is gradual accumulation of negative charges near the electrode. In order to observe more accurately space charge accumulation, the method called all-phases average is used. It consists in averaging all the space charge profiles in the 32 phase angles measured in one run [16].

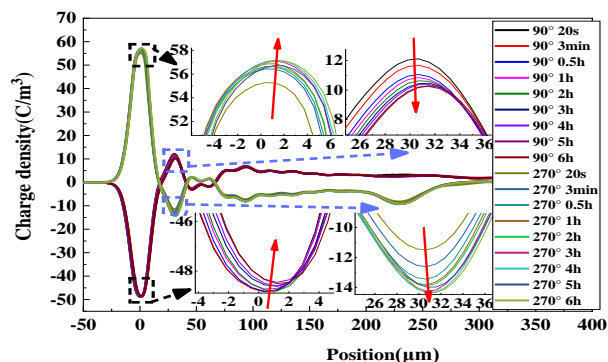


Figure 1. Measured charge density profiles at  $90^\circ$  and  $270^\circ$  in the process of applying an ac electric for 6 hours.

In the averaging process, the periodic charges at the interface whose polarity and amplitude change with time along the period are cancelled out, and non-periodic space charges that do not change with the phase are obtained. The curves of the all-phases averaged charge distribution of XLPE cable slices under ac electric field for 6 hours are shown in Figure 2.

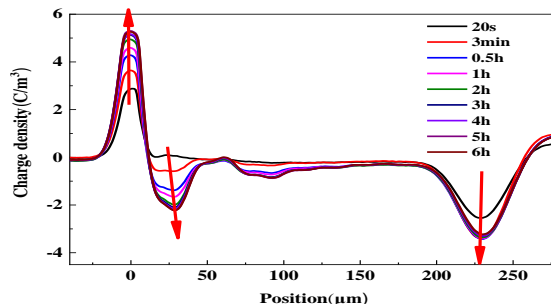


Figure 2. All-phases average space charge profiles recorded for 6 h under ac stress.

It can be seen from Figure 2 that the density of negative charges gradually increases at around 25  $\mu\text{m}$  away from the left electrode. At the left electrode interface, the positive image charge increases monotonically. The image charge at the right electrode, being negative, also increases. This behavior is more difficult to explain. One reason is the charges attenuation at the upper electrode in Figure 1. Besides, the upper semiconducting electrode may not behave as a pure conducting electrode under ac stress, which affects charges distribution into the semiconductor electrode and makes the electroacoustic signal response attenuate.

It is found that mainly negative charges accumulate in the material. According to the researches performed under dc electric field, the transport of positive negative charges is clearly different. Under ac, if charges injected during the positive voltage half cycle and those of opposite polarity injected during the negative half cycle cannot be completely recombined, there will be residual charges at the end of an ac period. Therefore, the space charges accumulation is speculated to be a consequence of the difference between positive and negative charges dynamics.

In order to verify this conjecture, a bipolar space charge transport model with symmetrical or asymmetrical parameters under ac electric field has been developed. The influence of physical parameters for charge accumulation are also studied.

### 3 BIPOLAR SPACE CHARGE TRANSPORT MODEL

The bipolar space charge model describes the dynamic of space charges in the insulating materials under electric field, as shown in Figure 3 [12]. The model assumes that there are four kinds of charges in the insulating material, which are free electrons, free holes, trapped electrons, and trapped holes. Free electrons and free holes are injected from cathode and anode respectively. They migrate inside the material under the action of electric field and can get trapped. If trapped charges have gained enough energy, they will de-trap and become free charges again. Recombination occurs between charges with opposite polarity.

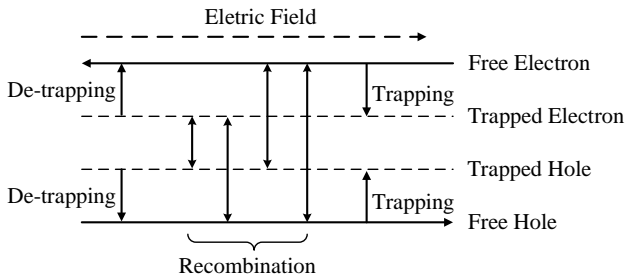


Figure 3. Schematic diagram of bipolar charge behavior.

#### 3.1 CHARGE TRANSPORT PROCESS

The traps are divided into shallow traps and deep traps, accounting respectively for conduction and long-lasting charge trapping. The trapping time of charges in shallow traps is relatively short. Therefore, they migrate through jump in shallow traps. If captured by deep traps, it is difficult for charges to escape, leading

to a long trapping time. This process plays a leading role in the recombination and accumulation of charges. In this model, a single-level of traps is used to simulate deep trapping level. Charge mobilities are set so as to take into account the jump of charges between shallow traps, to realize the charge conduction. The trapping coefficients and de-trapping barrier heights define the processes of capture and de-trapping of charges. The above processes can be described by three equations: transport equation, Poisson's equation and current continuity equation, as follows [18].

Transport equation:

$$J = \mu_{e,h} n_{e,h} E \quad (1)$$

Poisson's equation:

$$\nabla^2 V = \frac{\partial^2 V}{\partial x^2} = -\frac{\rho}{\epsilon_0 \epsilon_r} \quad (2)$$

$$E = -\nabla V \quad (3)$$

Current continuity equation:

$$\frac{\partial n_a}{\partial t} + \frac{\partial j_a}{\partial x} = S_a \quad (4)$$

where  $\rho$  is the net charge density of four charges;  $n_a$  is the charge density of each type of charge;  $j_a$  is the current density of free electrons and free holes.  $\epsilon_0$  is the vacuum dielectric constant,  $\epsilon_r$  is the relative permittivity. The  $S_a$  on the right side of the current continuity equation is the source term. They indicate the changes of the respective densities caused by the interaction between four kinds of charges, excluding those caused by migration [18]. The specific content is as follows:

$$s_e = -R_{eh} n_e n_h - R_{eht} n_e n_{ht} - T_e n_e \left(1 - \frac{n_{et}}{n_{0et}}\right) + v \exp\left(\frac{-\psi_{et}}{kT}\right) n_{et} \frac{n_{et}}{n_{0et}} \quad (5)$$

$$s_h = -R_{eh} n_e n_h - R_{eht} n_e n_{ht} - T_h n_h \left(1 - \frac{n_{ht}}{n_{0ht}}\right) + v \exp\left(\frac{-\psi_{ht}}{kT}\right) n_{ht} \frac{n_{ht}}{n_{0ht}} \quad (6)$$

$$s_{et} = -R_{eht} n_{et} n_h - R_{eth} n_{et} n_{ht} + T_e n_e \left(1 - \frac{n_{et}}{n_{0et}}\right) - v \exp\left(\frac{-\psi_{et}}{kT}\right) n_{et} \frac{n_{et}}{n_{0et}} \quad (7)$$

$$s_{ht} = -R_{eht} n_e n_{ht} - R_{eth} n_{et} n_{ht} + T_h n_h \left(1 - \frac{n_{ht}}{n_{0ht}}\right) - v \exp\left(\frac{-\psi_{ht}}{kT}\right) n_{ht} \frac{n_{ht}}{n_{0ht}} \quad (8)$$

Where  $s_e$ ,  $s_h$ ,  $s_{et}$ ,  $s_{ht}$  respectively indicate the rate of change in the density of free electrons, free holes, trapped electrons, and trapped holes,  $n_e$ ,  $n_h$ ,  $n_{et}$ ,  $n_{ht}$  respectively represent the density of free electrons, free holes, trapped electrons, and trapped holes.  $R$  represent the recombination coefficients between charges of opposite polarity,  $n_{0et}$  and  $n_{0ht}$  are the deep trap densities of electrons and holes.  $T_e$  and  $T_h$  represent the trapping coefficient of electrons and holes,  $v$  is the de-trapping rate,  $\psi_{et}$  and  $\psi_{ht}$  are respectively the de-trapping barrier heights for trapped electrons and trapped holes.

#### 3.2 INJECTION AND EXTRACTION OF CHARGES

The charges generated by ionization under high electric field are not considered, and charges in the insulating material all arise from injection at each electrode. The considered electric field intensity is much lower than 100 kV/mm, so the Schottky injection law is adopted [11]:

$$J = AT^2 \exp\left(-\frac{\psi_{e,h}}{kT}\right) \exp\left(\frac{e}{kT} \sqrt{\frac{eE}{4\pi\epsilon_0\epsilon_r}}\right) \quad (9)$$

Where  $A$  is the Richardson constant,  $T$  is the temperature,  $\psi_e$  and  $\psi_h$  are the injection barrier heights for electrons and holes,  $k$  is the Boltzmann's constant,  $e$  is the elementary electronic charge,  $E$  is the electric field intensity at the electrode.

The extraction of charges at the opposite electrode is done without barrier, obeying the transport equation.

### 3.3 MODEL CONFIGURATION

The thin-sheet XLPE insulation sample with a thickness of 230  $\mu\text{m}$  is described using a one-dimensional simulation model. The ground at 0  $\mu\text{m}$  is the lower electrode, and the sinusoidal ac voltage is applied at 230  $\mu\text{m}$  which is the upper electrode as shown in Figure 4. The applied voltage used in the simulation is  $V(t) = V_p \sin(2\pi ft)$ . The frequency  $f$  is 50 Hz and the peak value of voltage  $V_p$  is 8.05 kV. The resolution of the model has been achieved using Comsol software.

Eight physical parameters (four for each free charge type) play major roles on the dynamic behavior of space charge [11]. They are injection barrier height, mobility, trapping coefficient and de-trapping barrier height for each type of charge. In order to explore how to set the parameters of the simulation model under ac electric field to meet the experimental reality, the bipolar charge transport model has been resolved with symmetric and asymmetric parameters.

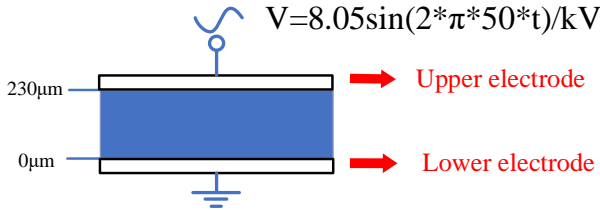


**Figure 4.** Applied voltage protocol used in the simulations. The ground at 0  $\mu\text{m}$  is the lower electrode, and the sinusoidal ac voltage is applied at 230  $\mu\text{m}$  which is the upper electrode.

## 4 SIMULATION RESULTS WITH SYMMETRICAL PARAMETERS

### 4.1 SETTING OF SYMMETRICAL PARAMETERS

The physical-parameters used in the simulations may have a great influence on the level of charge accumulation. These parameters are however not available in the literature, and are mostly obtained from experimental measurement or simulation and experimental fitting. In order to see the impact of these parameters on the net charge density under ac electric field, simulations have first been performed with symmetrical parameters. The parameters setting in this model is based on the values published in the literature [12-15 ,19, 20], and are presented in Table 1. Table 1 also presents the other fixed parameters used in the simulations.

**Table 1.** Setting of symmetrical parameters used in the simulations.

Parameter	Value
$\psi_{e,h}$ (injection barrier heights)	1.2 eV

$\psi_{et,ht}$ (de-trapping barrier heights)	0.97 eV
$\mu_{e,h}$ (mobilities)	$1 \times 10^{-12} \text{ m}^2 \text{ V}^{-1} \text{ s}^{-1}$
$T_{e,h}$ (trapping coefficients)	$0.1 \text{ s}^{-1}$
$R_{eht,eth,ethh}$ (recombination coefficients for other than between free electrons/free holes)	$4 \times 10^{-3} \text{ m}^3 \text{ C}^{-1} \text{ s}^{-1}$
$R_{e,h}$ (recombination coefficients between free electrons and free holes)	0
$n_{0et,0ht}$ (trap densities)	$5.9 \times 10^{20} \text{ m}^{-3}$
$\nu$ (de-trapping rate)	$6 \times 10^{12} \text{ s}^{-1}$
$\epsilon_r$ (relative permittivity)	2.3

## 4.2 SPACE CHARGE ACCUMULATION CHARACTERISTICS WITH SYMMETRICAL PARAMETERS

Figure 5 presents the simulated net space charge density profiles, at the phase of  $90^\circ$  for times varying from 0 to 60 minutes. All parameters being symmetric, the net charge variation is small, as the charge density at each time almost overlap. Hence, the charge density curves at the electrode are amplified. The maximal space charge density at the electrode interface is around  $0.0013 \text{ C/m}^3$ . The increase of charge density with time is not monotonic, but fluctuates in a very small range. The space charge evolution at the upper electrode and the lower electrode is basically symmetrical. Even if the net charge density is almost zero, the maximal penetration depth within the material for free charge is around 6  $\mu\text{m}$ , with the chosen symmetrical parameters. This is not observable on the net charge density profiles, but is easily available with the simulation. From Figure 5, there is no obvious accumulation of space charges under ac electric field with symmetrical parameters. Charge accumulation in the simulation results with symmetric parameters is obviously inconsistent with the experimental results.

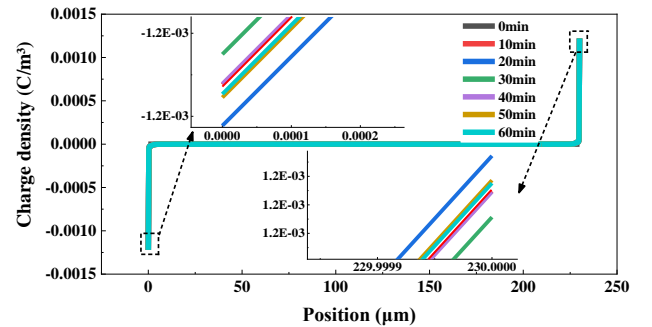


**Figure 5.** Space charge density profiles, at  $90^\circ$  within 60 minutes with symmetrical parameters.

## 5 SIMULATION RESULTS WITH ASYMMETRICAL PARAMETERS

### 5.1 SETTING OF ASYMMETRICAL PARAMETERS

Most of the researches published on the bipolar charge transport model propose asymmetrical parameters for electrons and holes. The injection barrier is obtained by measuring the threshold electric field of the charge injection or the current density [19]. According to the references, the injection barrier of free electrons is lower than that of free holes [20, 21]. The

mobility of free charges can be deduced from experiment [22]. Some researchers consider that the mobility of negative charges is larger than that of positive charges [22, 23, 24]. The trapping coefficients of free charges mostly come from the comparison of simulation and experiment. At present, the trapping coefficient of free holes is chosen generally larger than that of free electrons [20,21,23]. The de-trapping barrier height can be calculated according to the first principles [25] or can be obtained by experimental evaluation of the depolarization characteristics of space charges [20]. It is assumed that the de-trapping barrier height of the trapped holes is higher than that of the trapped electrons [20,21,24]. The settings of the asymmetrical parameters chosen for our simulations are shown in Table 2 and the other fixed parameters are given in Table 1.

**Table 2.** Setting of asymmetrical parameters.

Parameter	Value
$\psi_{e,h}/eV$ (injection barrier heights)	1.19, 1.21
$\psi_{et,ht}/eV$ (de-trapping barrier heights)	0.95, 0.97
$\mu_{e,h}/(m^2V^{-1}s^{-1})$ (mobilities)	$3 \times 10^{-12}, 1 \times 10^{-12}$
$T_{e,h}/(s^{-1})$ (trapping coefficients)	0.05, 0.1

## 5.2 SIMULATION OF SPACE CHARGE ACCUMULATION WITH ASYMMETRICAL PARAMETERS

The simulation protocol is the same as that with symmetrical parameters in Figure 4. Figure 6 shows the net charge density profiles, at the phase of  $90^\circ$ , for different times under ac voltage, ranging from 0 to 60 minutes. Positive charges accumulate near the interface of the two electrodes, while the negative charges accumulate at about  $15 \mu m$  away from the electrodes. The density of the two kinds of charges increases monotonously with the time. The simulated negative charge accumulation is consistent with experiment result at the lower electrode. The positive charge stays close to the electrode and cannot be resolved experimentally given the current resolution. Due to signal attenuation in experimental results of Figure 1, the simulation and the experimental results cannot be compared at the upper electrode. However, it must be noted that in principle, phenomena are symmetrical under ac stress. Therefore, focus can be put on features at one electrode.

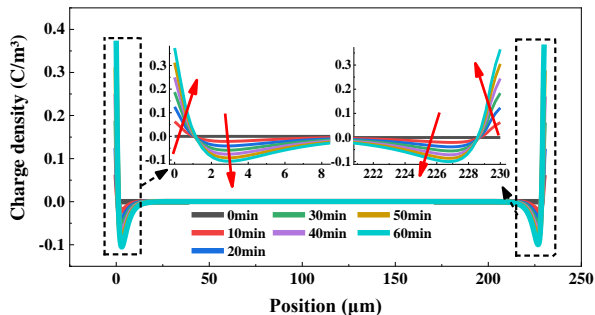


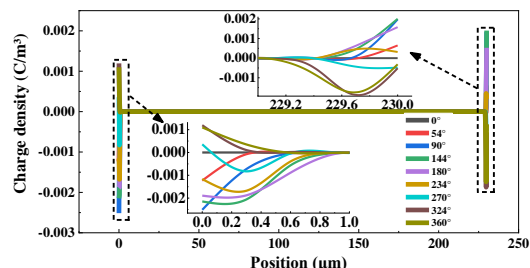
**Figure 6.** Net charge density profiles, at  $90^\circ$  within 60 minutes with asymmetrical parameters.

The simulation time is shorter and the level of charge accumulation is lower than the experimental one. However, the trends at the lower electrode are the same, i.e. an accumulation

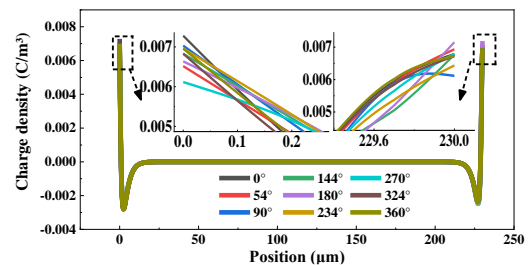
of negative charges. The penetration depth for negative charge is not exactly the same, but one could think that after 6 hours in the simulation, negative charges should penetrate deeper inside the material. However, it is difficult to conclude for the positive charges observed in the simulation, as they are too close to the electrode to be detected experimentally, and would be included in the image charges at the electrode. The favorable comparison between experiment and simulation however validates the model and the chosen asymmetrical parameters.

## 5.3 PHASE CHARACTERISTICS OF SPACE CHARGE WITH ASYMMETRICAL PARAMETERS

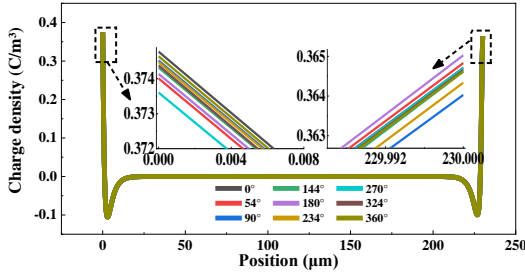
In order to explore the detailed process of charge accumulation, the space charge density profiles as a function of phase during one period is presented in Figure 7 at stressing time  $t=0min$  (Figure 7a),  $t=1min$  (Figure 7b), and  $t=60min$  (Figure 7c). Figure 7a shows the evolution of space charge in the first voltage cycle (0-0.02 seconds). Negative charges are injected when the lower electrode is the cathode (phase  $0^\circ$ - $180^\circ$ ), while positive charges are injected when the lower electrode is the anode ( $180^\circ$ - $360^\circ$ ). However, negative charges remain inside the material, even for the second half of the voltage cycle. Even after 1 min (Figure 7b), positive charges accumulate at the interface, while negative charges are located deeper in the bulk. Because space charges are injected and extracted under the action of electric field, the amplitude of space charges at the electrode interface still varies with the phase. However, due to the increasing amount of space charge accumulated, injection, extraction and transport are not enough to change the polarity of space charges near the electrode, and they only slightly change the amplitude of charge density.



(a) 0 minutes



(b) 1 minute



(c) 60 minutes

**Figure 7.** The space charge density with symmetry parameters changes with the phases in a voltage cycle.

Figure 7c shows the distribution of space charge density with phase at 60 minutes. Relative to the time of 1 minute, the maximum density of positive space charges at the electrode interface increases from  $0.007 \text{ C/m}^3$  to  $0.38 \text{ C/m}^3$ , and the maximum density of negative space charges at the deeper part of the material increases from  $0.003 \text{ C/m}^3$  to  $0.1 \text{ C/m}^3$ . There is an obvious accumulation of space charges. Moreover, due to the increase of charge accumulation level, the charge density curves of all phases are almost identical, and the change of charge density near the electrode interface caused by injection and extraction is less obvious than that at 1 minute.

According to the above analysis, the proposed model with asymmetric parameters enables having an increasing charge accumulation with simulation time. The gradual accumulation of space charges is mainly due to the chosen parameters, i.e. a relatively low mobility, a deep trapping level with a low probability to de-trapping for holes, which implies that positive charges are retained near the electrode interface while the negative charges penetrate inside the material during each voltage period. The variation of the net charge density is less visible when enough charges have been accumulated. Actually, the density of space charges is always fluctuating slightly with the polarity and amplitude of the voltage due to the space charges dynamic.

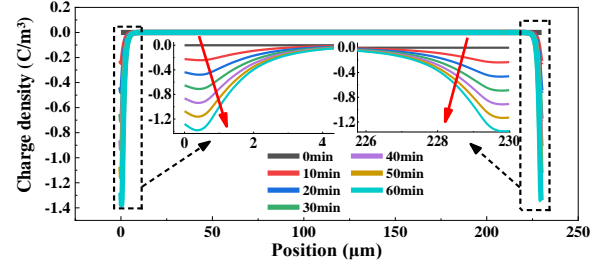
## 6 DISCUSSION

Asymmetrical parameters enhance charge accumulation as shown in Figure 6, which is the result of the impact of the injection barrier, mobility, trapping coefficient, and de-trapping barrier. These four parameters play a major role in the charge motion mechanism from different angles. Therefore, we need to discuss the influence of each parameter separately. In the following, only one of the parameters is set asymmetrically at the same time, the other parameters are kept symmetrical and are those of Table 1.

Figure 8a shows the effect of injection barriers height on space charge accumulation, injection barriers for electrons and holes are set as  $1.19 \text{ eV}$  and  $1.21 \text{ eV}$  respectively. When the injection barrier for electrons is lower than that of holes, negative charges gradually accumulate at the two electrodes, and no positive charges are observed next to each electrode (as in Figure 6). The density of accumulated charge reaches  $1.4 \text{ C/m}^3$  after 60 minutes under ac electric field. This is due to the fact that the number of injected electrons is larger than that of

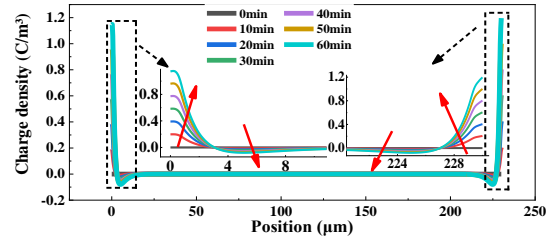
holes, which is one of the important reasons for the accumulation of negative charges in the material.

Figure 8b shows the impact of the mobility value on charge distribution. In this case, the electron mobility is set to  $3 \times 10^{-12} \text{ m}^2\text{V}^{-1}\text{s}^{-1}$  while the one for holes is kept at  $1 \times 10^{-12} \text{ m}^2\text{V}^{-1}\text{s}^{-1}$ , the other parameters being symmetrical. It can be seen that positive charges gradually accumulate at the electrode interface while negative charges accumulate deeper in the bulk of the material.

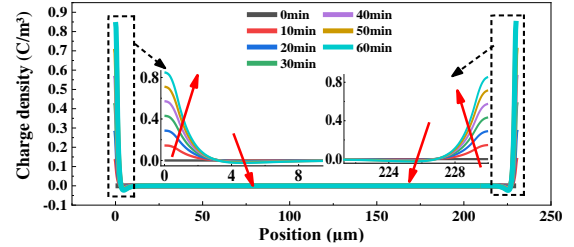


(a) Impact of the injection barriers height value on the net charge density.

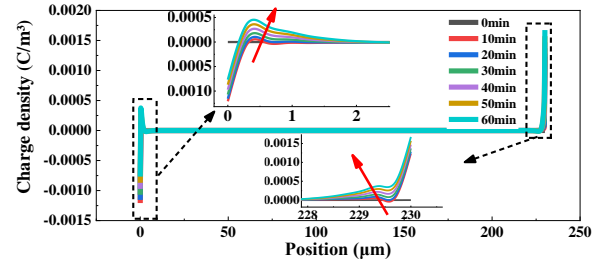
$\psi_e = 1.19 \text{ eV}$ ,  $\psi_h = 1.21 \text{ eV}$ . Other parameters of Table 1.



(b) Impact of the mobility value on the net charge density.  $\mu_e = 3 \times 10^{-12} \text{ m}^2\text{V}^{-1}\text{s}^{-1}$ ,  $\mu_h = 1 \times 10^{-12} \text{ m}^2\text{V}^{-1}\text{s}^{-1}$ . Other parameters of Table 1.



(c) Impact of the trapping coefficient on the net charge density.  $T_e = 0.05 \text{ s}^{-1}$ ,  $T_h = 0.1 \text{ s}^{-1}$ . Other parameters of Table 1.



(d) Impact of the de-trapping coefficient on the net charge density.  $\psi_{et} = 0.95 \text{ eV}$ ,  $\psi_{ht} = 0.97 \text{ eV}$ . Other parameters of Table 1.

**Figure 8.** Space charge density profiles at  $90^\circ$  within 60 minutes when the one of parameters is asymmetrical.

The accumulation level of positive charges is greater than that of negative charges. This is because the mobility of the positive charges is lower than that of the negative charges, which makes

it difficult for positive charges to completely recombine with negative charges deeper in the material.

Figure 8c presents the impact of the trapping coefficient on the net charge density, the trapping coefficients being set to  $0.05\text{s}^{-1}$  for electrons and  $0.1\text{s}^{-1}$  for holes, the other parameters being those of Table 1. The effect of trapping coefficient on charge accumulation is similar to that of mobility. It also leads to the accumulation of positive charges at the electrode interface and negative charges inside the material. But the density of accumulated charge is lower than that in Figure 8b. Both trapping coefficient and mobility limit the internal movement of positive charges. The difference is that mobility limits the velocity of charges motion while the trapping coefficient limits the quantity of charges.

Figure 8d shows the impact of the de-trapping parameter on the net charge density. In this case, the de-trapping barriers of trapped electrons and trapped holes are 0.95 eV and 0.97 eV respectively. The asymmetry of the de-trapping barrier leads to the decrease of negative charges at the lower electrode and the increase of positive charges at the upper electrode at the phase of  $90^\circ$ . Some positive charges even accumulate at the lower electrode.

In summary, due to the lower injection barrier and higher mobility of free electrons, more negative charges are injected and migrate deeper into the material under the action of electric field. Due to the larger trapping coefficient of free holes and the higher de-trapping barrier of trapped holes, free holes are more likely to be captured by the traps at the electrode interface. The charges with opposite polarities injected during the positive and negative half cycles are not easily neutralized or extracted. Therefore, the negative charges remain inside the insulation and the positive charges accumulate near the surface.

## 7 CONCLUSION

From the charge measurement experiment under ac electric field, it is found that negative charges accumulate inside the material. The cause of charge accumulation is speculated to be the difference of positive and negative charge movement mechanism. In order to verify this speculation, a bipolar space charge transport model with asymmetrical parameters has been tested, providing space charge characteristics as a function of depth, phase, and stressing time of XLPE under ac electric field. Through the results of long-time space charge accumulation and charge variation with phases of single-period, asymmetrical model is verified to be applicable for space charge simulation under ac stress.

Positive charges accumulate near the electrode interface and negative charges accumulate in the deeper part of the materials. The significant reason for charge accumulation is residual charges in each ac period caused by the asymmetrical parameters of positive and negative charges. The space charge density in the vicinity of the electrodes increases with running time, which results in charge variation with phase caused by injection and extraction less obvious.

As expected, there is not obvious space charge accumulation with symmetrical parameters. The asymmetry of the injected barriers, mobilities, trapping coefficients and de-trapping

barriers affects the motion mechanism of positive and negative charges from different aspects and levels, acting either on the velocity or the number of charges. The study is helpful to research charge accumulation mechanism of insulation materials under ac stress.

## ACKNOWLEDGMENT

The research work of this paper was financed by the Shandong Provincial Natural Science Foundation (Grant No. ZR2019QEE013) and the National Natural Science Foundation of China (Grant No.51907105). I would like to express my heartfelt thanks to them.

## REFERENCES

- [1] G. C. Montanari, "Bringing an insulation to failure: the role of space charge," *IEEE Trans. Dielectr. Electr. Insul.*, vol. 18, no. 2, pp. 339-364, Apr. 2011.
- [2] T. Tanaka, "Charge transfer and tree initiation in polyethylene subjected to AC voltage stress," *IEEE Trans. Electr. Insul.*, vol. 27, no. 3, pp. 424-431, Jun. 1992.
- [3] D. He *et al.*, "The influence mechanism of semiconductive material on space charge accumulation in HVDC cable accessory," *IEEE Trans. Dielectr. Electr. Insul.*, vol. 26, no. 5, pp. 1479-1486, Oct. 2019.
- [4] F. Baudoin *et al.*, "Bipolar charge transport model with trapping and recombination: An analyze of the current vs. applied electric field characteristic," 2007 IEEE International Conference on Solid Dielectrics, Winchester, 2007, pp. 19-22.
- [5] A. Beldjilali, N. Saidi-Amroun, and M. Saidi, "Space charge modeling in polymers: review of external applied constraints effects," *IEEE Trans. Dielectr. Electr. Insul.*, vol. 23, no. 1, pp. 573-585, Feb. 2016.
- [6] C. Thomas, G. Teyssedre, and C. Laurent, "Space-charge dynamic in polyethylene: from dc to ac stress," *J. Appl. Phys.*, vol. 44, no. 1, pp. 015401, Dec. 2011.
- [7] C. Thomas, G. Teyssedre, and C. Laurent, "A new method for space charge measurements under periodic stress of arbitrary waveform by the pulsed electro-acoustic method," *IEEE Trans. Dielectr. Electr. Insul.*, vol. 15, no. 2, pp. 554-559, Apr. 2008.
- [8] G. Chen *et al.*, "ac aging and space-charge characteristics in low-density polyethylene polymeric insulation," *J. Appl. Phys.*, vol. 97, no. 8, pp. 083713-083713-7, Apr. 2005.
- [9] S. Bamji, M. A. Dakka, and A. Bulinski, "Phase-resolved pulsed electro-acoustic technique to detect space charge in solid dielectrics subjected to AC voltage," *IEEE Trans. Dielectr. Electr. Insul.*, vol. 14, no. 1, pp. 77-82, Feb. 2007.
- [10] D. He *et al.*, "Space charge characteristics of power cables under AC stress and temperature gradients," *IEEE Trans. Dielectr. Electr. Insul.*, vol. 23, no. 4, pp.2404-2412, Aug. 2016.
- [11] J. M. Alison and R. M. Hill, "A model for bipolar charge transport, trapping and recombination in degassed crosslinked polyethylene," *J. Appl. Phys.*, vol. 27, no. 6, pp. 1291-1299, Jun. 1994.
- [12] J. Zhao *et al.*, "Numeric description of space charge in polyethylene under ac electric fields," *J. Appl. Phys.*, vol. 108, no. 12, pp. 124107-124107-7, Dec. 2010.
- [13] F. Baudoin *et al.*, "Modeling electroluminescence in insulating polymers under ac stress: effect of excitation waveform," *J. Appl. Phys.* vol. 44, no. 16, pp. 165402, Apr. 2011.
- [14] S. Le Roy, G. Teyssedre, and C. Laurent, "Modelling space charge in a cable geometry," *IEEE Trans. Dielectr. Electr. Insul.*, vol. 23, no.4, pp. 2361-2367, Aug. 2016.
- [15] Y. Zhan, G. Chen, and M. Hao, "Space charge modelling in HVDC extruded cable insulation," *IEEE Trans. Dielectr. Electr. Insul.*, vol. 26, no.1, pp. 43-50, Feb. 2019.
- [16] D. He *et al.*, "Space charge behavior in XLPE cable insulation under ac stress and its relation to thermo-electrical aging," *IEEE Trans. Dielectr. Electr. Insul.*, vol. 25, no. 2, pp. 541-550, Apr. 2018.
- [17] C. Gao *et al.*, "A Study on the Space Charge Characteristics of AC Sliced XLPE Cables," *IEEE Access*, vol. 7, pp. 20531-20537, 2019.



- [18] S. Le Roy *et al.*, "Description of bipolar charge transport in polyethylene using a fluid model with a constant mobility: model prediction," *J. Appl. Phys.*, vol. 37, no. 2, pp. 298, Jan. 2004.
- [19] L. Lan *et al.*, "Effect of temperature on space charge trapping and conduction in cross-linked polyethylene," *IEEE Trans. Dielectr. Electr. Insul.*, vol. 21, no. 4, pp. 1784-1791, Aug. 2014.
- [20] J. Wu *et al.*, "Simulation of space charge behavior in LDPE with a modified of bipolar charge transport model," *Proceedings of 2014 International Symposium on Electrical Insulating Materials*, Niigata, Japan, 2014, pp. 65-68.
- [21] J. Wu, "Experimental study and numerical simulation of charge transport in low density polyethylene nanocomposite medium," (In Chinese) PhD dissertation, Shanghai Jiao Tong University, Shanghai, 2012.
- [22] G. Zhou *et al.*, "Investigation of charge transport in LDPE/SiO<sub>2</sub> Nanocomposite based on the simultaneous observation of charge and current behaviour," *IEEE Trans. Dielectr. Electr. Insul.*, vol. 26, no. 6, pp. 1981-1988, Dec. 2019
- [23] A. Hoang, Y. Serdyuk, and S. Gubanski, "Charge Transport in LDPE Nanocomposites Part II—Computational Approach," *Polymers*, vol. 8, no. 4, pp. 103, Mar. 2016.
- [24] D. Min *et al.*, "Charge transport properties of insulators revealed by surface potential decay experiment and bipolar charge transport model with genetic algorithm," *IEEE Trans. Dielectr. Electr. Insul.*, vol. 19, no. 6, pp. 2206-2215, Dec. 2012.
- [25] M. Meunier *et al.*, "Molecular modeling of electron traps in polymer insulators: Chemical defects and impurities," *J. Chem. Phys.*, vol. 115, no. 6, pp. 2876-2881, Aug. 2001.



**Dongxin He** was born in Weifang City, China, in 1990. He received the B.S. degree in electrical engineering from Shandong University. He then enrolled in North China Electric Power University in Beijing and obtained the Ph.D. degree. In 2015, he travelled to the Laboratory of Plasma and Energy Conversion (LAPLACE) in Toulouse, France, as a visiting scholar. Currently, he is a lecturer in Shandong University, Jinan, China. As a researcher, His current research interests include condition monitoring and fault diagnosis of power equipment, space charge in polymer materials especially in cable insulation under ac stress.



**Zhe Xu** was born Qingdao, China. She received the B.S. degree from China University of Petroleum, Qingdao, China, in 2020. She is currently pursuing the master's degree in electrical engineering in Shandong University, Shandong, China. Her current research interests include space charge in polymer materials.



**Hongshun Liu** was born in Qingdao, China. He received the B.Sc. and Ph.D. degree in electrical engineering from Shandong University, Shandong, China, in 2004 and 2010, respectively.

Currently, he is a lecturer of Electrical Engineering at Shandong University, Shandong, China. His research interests include the modeling and simulation for power system electromagnetic transient processes, overvoltage and insulation coordination, condition monitoring and intelligent systems, high-voltage power electronics, etc.

Dr. Liu is a member of the Institution of Engineering and Technology (IET) and the Chinese Society of Electrical Engineering (CSEE).

**Qingjing Zang** was born Weifang, China. He received the B.S. degree from Shandong University, Jinan, China, in 2020.

He is currently pursuing the master's degree in electrical engineering in Shandong University, Shandong, China. His current research interests Real-time monitoring technology of transformer hot spot temperature based on ultrasonic wave.



**Qingquan Li** was born in Laiwu city, Shandong Province, China, in 1969. He received the Ph.D. degrees in electrical engineering from Xi'an Jiaotong University, Xi'an, China, in 2003. Currently, he is a professor at Shandong University, Jinan, China. His research interests include the lightning protection and grounding technology, the high voltage insulation and measurement technology, and the detection and diagnosis techniques for electrical equipment.



**Séverine Le Roy** was born in Belfort, France. She graduated in molecular and structural physical chemistry in 2001 at the Joseph Fourier University, Grenoble, France. Then she joined the Electrical Engineering Laboratory in Toulouse and obtained her Ph.D. degree in electrical engineering in 2004 from Paul Sabatier University. She entered the CNRS (National Centre of Scientific Research) in 2006. She is now dealing with modelling activities in relation with charge transport and ageing, for various domains of applications like electrical engineering, spatial environment. She is also concerned in the relationship between experiments and simulations.



**Gilbert Teysedre** was born in May 1966 in Rodez, France. He received his Engineer degree in materials physics and graduated in solid state physics in 1989 at the National Institute for Applied Science (INSA). Then he joined the Solid-state Physics Lab in Toulouse and obtained the Ph.D. degree in 1993 for work on ferroelectric polymers. He entered the CNRS in 1995 and has been working since then at the Electrical Engineering Lab (now LAPLACE) in Toulouse. His research activities concern the development of luminescence techniques in

insulating polymers with focus on chemical and physical structure, degradation phenomena, space charge and transport properties. He is currently Senior Director at CNRS in a team working on the reliability of dielectrics in electrical equipment.